Supporting Information

SI Materials and Methods

Plant Treatments. For osmotic/salt treatments, sterilized seeds were germinated on half strength MS medium and seedlings were transferred to test plates four days after germination. For root length assays, germinated seedlings on control plates were placed vertically for one week and then transferred to plates supplemented with 30% PEG or 0.1 M NaCl. For soil drought tests, size matched plants were obtained by sowing wild type (Col-0) seeds, in the same pot, about 10 days later than the *mlk1 mlk2* double mutant seeds. Plants with similar leaf area were subject to water withholding for one week and then re-watered to examine their survival. For immunoblot and ChIP-Seq analyses, sterilized seeds were sown directly on Whatman filter paper set on MS plates. Three-week-old seedlings were then transferred, with the Whatman paper as support, to control MS plates or to plates containing 30% PEG for different periods of time.

***In Vitro* Protein Kinase Activity Assay.** The open reading frame (ORF) of *MLK1*, amplified by RT-PCR with the primers listed in Table S3, was cloned into the pSTBlue-1 (Novagen) vector. After sequence verification, the ORF was ligated into the *Not*I and *Bam*HI sites of the pMAL-c5X vector (NEB), for expression as a fusion with maltose-binding protein (MBP). The fusion protein was produced in the E. *coli* BL21(DE3) strain, by induction with 0.1 mM IPTG for 16 hours, and purified with Amylose Resin (NEB). Protein kinase activity was assayed as described (1), using histone H3 or an unmodified histone H3 peptide (residues 1-21) biotin conjugate (Upstate 12-403) as the substrates.

Cytological Analyses. Sample preparation for heterochromatin evaluation in nuclei was performed as previously described by Ross *et al.* (2) with minor modifications. Briefly, leaves were fixed in Ethanol:Acetic Acid (3:1) overnight. Fixed samples were washed and rinsed in citrate buffer (10 mM sodium citrate, pH 4.5) before removing cell walls by enzymatic digestion with 0.3% (w/v) each of cellulase, pectolyase and cytohelicase (Sigma) in 10 mM sodium citrate. Digested samples were rinsed and stained with 1 μg/ml BisBenzimide H33342 (Sigma, B2261) in staining buffer (PBS containing 1 mg/ml polyvinylpyrrolidone and 0.03% Triton X-100) for 20 minutes.

DNA Methylation Analyses. Genomic DNA was extracted from leaves and methylation status was assayed with methylation sensitive restriction endonucleases as previously described (1).

Microarray Assays. For transcript profiling by microarray hybridization, total RNA from rosette leaves from 3-week old wild type or *dm* plants was isolated by using TRI reagent (Molecular Research Center). Three independent experiments (replicates) were carried out. Fifteen μg of total RNA from each replicate were used to generate labeled cRNA for hybridization to the Arabidopsis ATH1 GeneChip following the manufacturer's protocol (Affymetrix). Microarray data were processed with the RMA and edgeR packages in Bioconductor.

ChIP-Seq Data Analysis. For examining the chromosomal distribution of epigenetic marks, all reads were aligned with SeqMap (3) to the Arabidopsis genome (TAIR 10), allowing no more than 2 mismatches, and normalized as Reads Per Kilobase per Million Mapped Reads (RPKM). Fold changes were calculated using the total number of normalized reads in windows of 100 kb. For the distribution of epigenetic marks associated with protein coding genes, all examined genes had annotated transcription start sites and were detectably expressed in our microarray assays (http://bioinformatics.unl.edu/ucsc/cgi-bin/hgGateway), using the Arabidopsis ATH1 GeneChip (Affymetrix). To minimize ambiguity introduced from adjacent chromosomal regions, the study was restricted to genes longer than 1 kb and separated by a distance of at least 1 kb from upstream and downstream neighboring genes. Additionally, surveyed genes were categorized into 3 subgroups based on their length: short genes (1-2 kb), intermediate genes (2-4 kb) and long genes (>4 kb). All genes were aligned at the transcription start sites or transcription end sites in each length group as described by Zhang *et al.* (4). The number of normalized reads in 100 bp windows within genes was counted and the fold change between different samples was calculated as previously described (5). For epigenetic mark distribution within transposable elements (TEs), TEs were divided into three groups according to their length (<2 kb, 2-4 kb, and > 4 kb) and aligned at their beginning (6). The transcribed region of each TE was split into 10 equal-length bins and the total number of normalized reads in each bin was counted. The coordinates of genes and TEs were obtained from TAIR 10 (http://www.arabidopsis.org).

1. Casas-Mollano JA, Jeong BR, Xu J, Moriyama H, & Cerutti H (2008) The MUT9p kinase phosphorylates histone H3 threonine 3 and is necessary for heritable epigenetic silencing in Chlamydomonas. *Proc Natl Acad Sci U S A* 105(17):6486-6491.
2. Ross KJ, Fransz P, & Jones GH (1996) A light microscopic atlas of meiosis in Arabidopsis thaliana. *Chromosome Res* 4(7):507-516.
3. Jiang H & Wong WH (2008) SeqMap: mapping massive amount of oligonucleotides to the genome. *Bioinformatics* 24(20):2395-2396.
4. Zhang X, Bernatavichute YV, Cokus S, Pellegrini M, & Jacobsen SE (2009) Genome-wide analysis of mono-, di- and trimethylation of histone H3 lysine 4 in Arabidopsis thaliana. *Genome Biol* 10(6):R62.
5. Govin J*, et al.* (2010) Genome-wide mapping of histone H4 serine-1 phosphorylation during sporulation in Saccharomyces cerevisiae. *Nucleic Acids Res* 38(14):4599-4606.
6. Wang X*, et al.* (2009) Genome-wide and organ-specific landscapes of epigenetic modifications and their relationships to mRNA and small RNA transcriptomes in maize. *Plant Cell* 21(4):1053-1069.

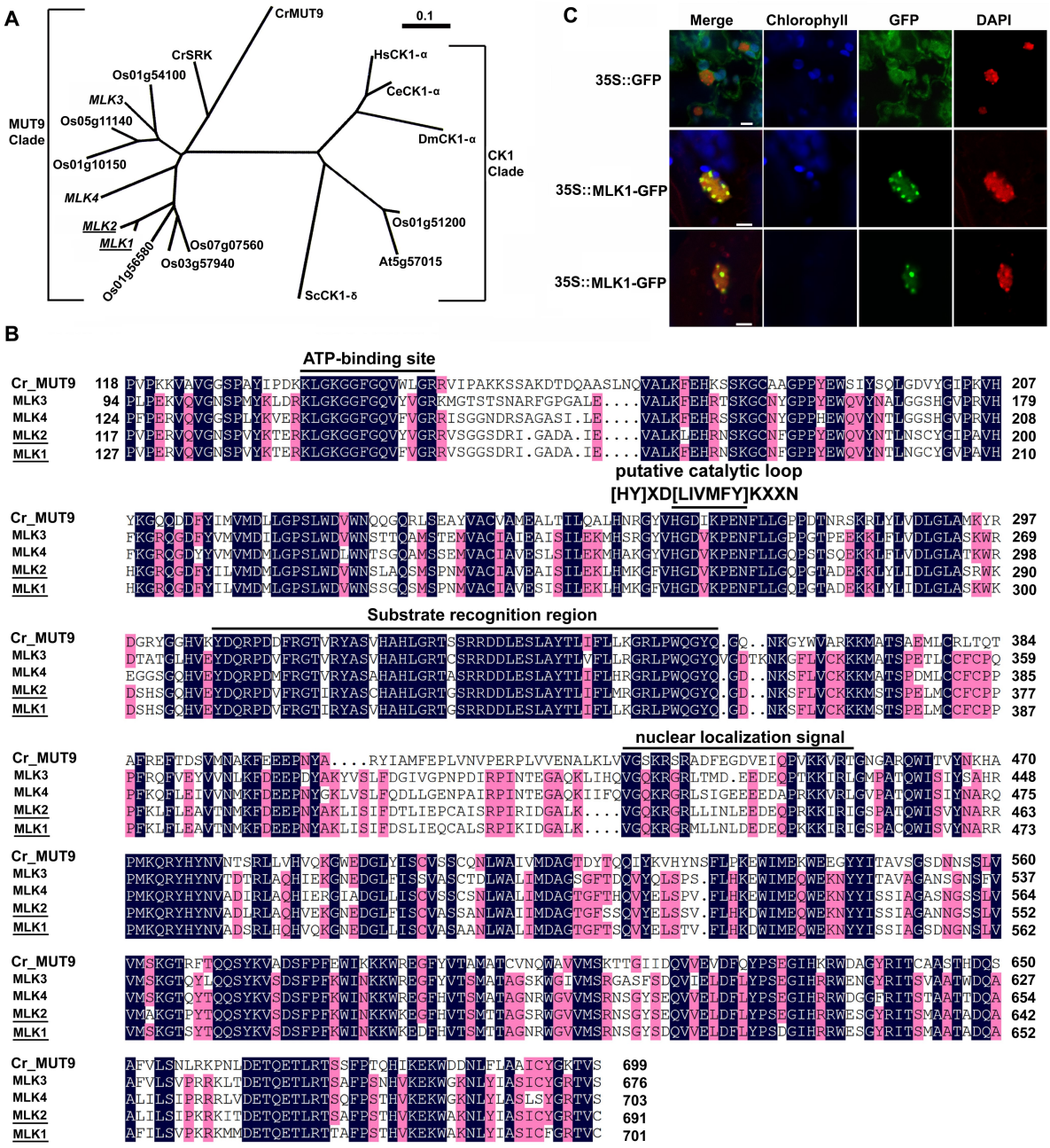

Fig. S1. Phylogenetic relationship of MUT9-related Ser/Thr protein kinases and subcellular localization of the MLK1-GFP fusion protein. (*A*) Neighbor-joining tree showing the phylogenetic relationship among MUT9 and related Ser/Thr protein kinases from several eukaryotes. The two kinases defective in the characterized Arabidopsis double mutant are underlined. Accession numbers of the proteins used to draw the tree have been previously reported (1). CK1, Casein Kinase 1; MLK1, At5g18190; MLK2, At3g03940; MLK3, At2g25760; MLK4, At3g13670. (*B*) Sequence alignment of Chlamydomonas MUT9 and its Arabidopsis homologs. Amino acid residues shaded in black or pink represent identical residues in 5 or 4 proteins, respectively. Key functional domains and the nuclear localization signal are indicated. The nuclear localization signal was predicted using cNLS Mapper (http://nls-mapper.iab.keio.ac.jp/cgi-in/NLS_Mapper_form.cgi). (*C*) Subcellular localization of the MLK1-GFP fusion protein, driven by the 35S CaMV promoter, in transgenic Arabidopsis. Representative pseudo-colored images of leaf cells are shown, with nuclei indicated by DAPI staining. Bar = 5 μm.

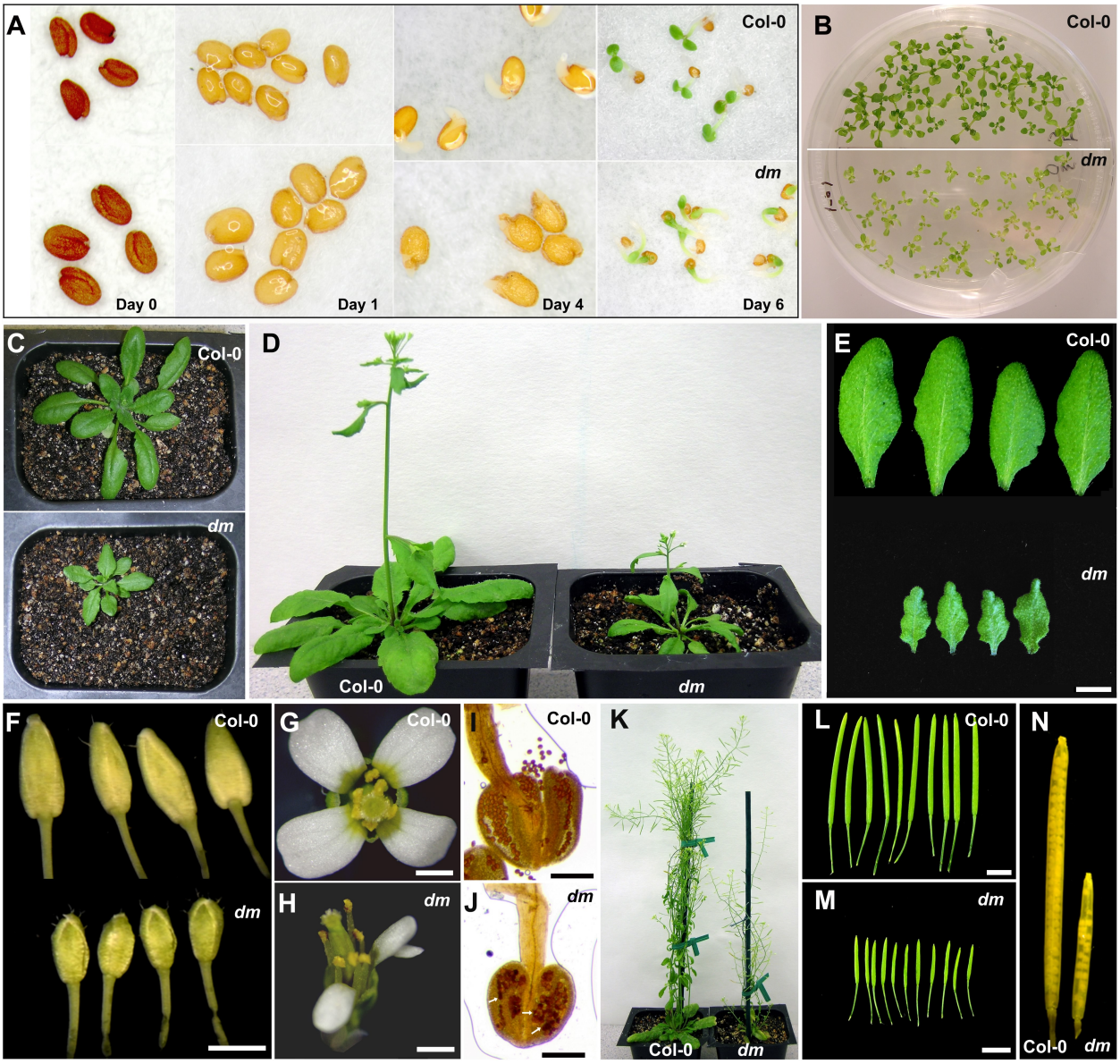

Fig. S2. Morphological phenotypes of the *mlk1 mlk2* double mutant. (*A*) Seed germination of the wild type (Col-0) and the *mlk1 mlk2* double mutant (*dm*). Mature seeds were germinated on water-imbibed Whatman filter paper and pictures taken at the indicated days. (*B*) Twelve-day old seedlings grown on half strength MS medium. The *dm* seedlings are smaller with pale-green leaves. (*C*) Three-week old plants grown in soil. (*D*) Flowering plants. (*E*) Fourth rosette leaves of flowering plants. The *dm* has curly leaves of small size. Bar = 1 cm. (*F*) Flower buds. The *dm* shows smaller and roundish buds. Bar = 0.1 cm. (*G*) Wild type flower. (*H*) Flower from the *dm*, showing abnormal reproductive organs. Bar = 0.1 cm. (*I-J*) Pollen grains from the wild type and the *dm* stained with 1% KI-I_2. Anthers from the *dm* have reduced number of pollen grains that are variable in size (indicated by arrows). Bar = 200 µm. (*K*) Mature plants. (*L-M*) Siliques from the wild type and the *dm*. Bar = 1 cm. (*N*) Seeds within mature siliques. Siliques were cleared with 75% ethanol.

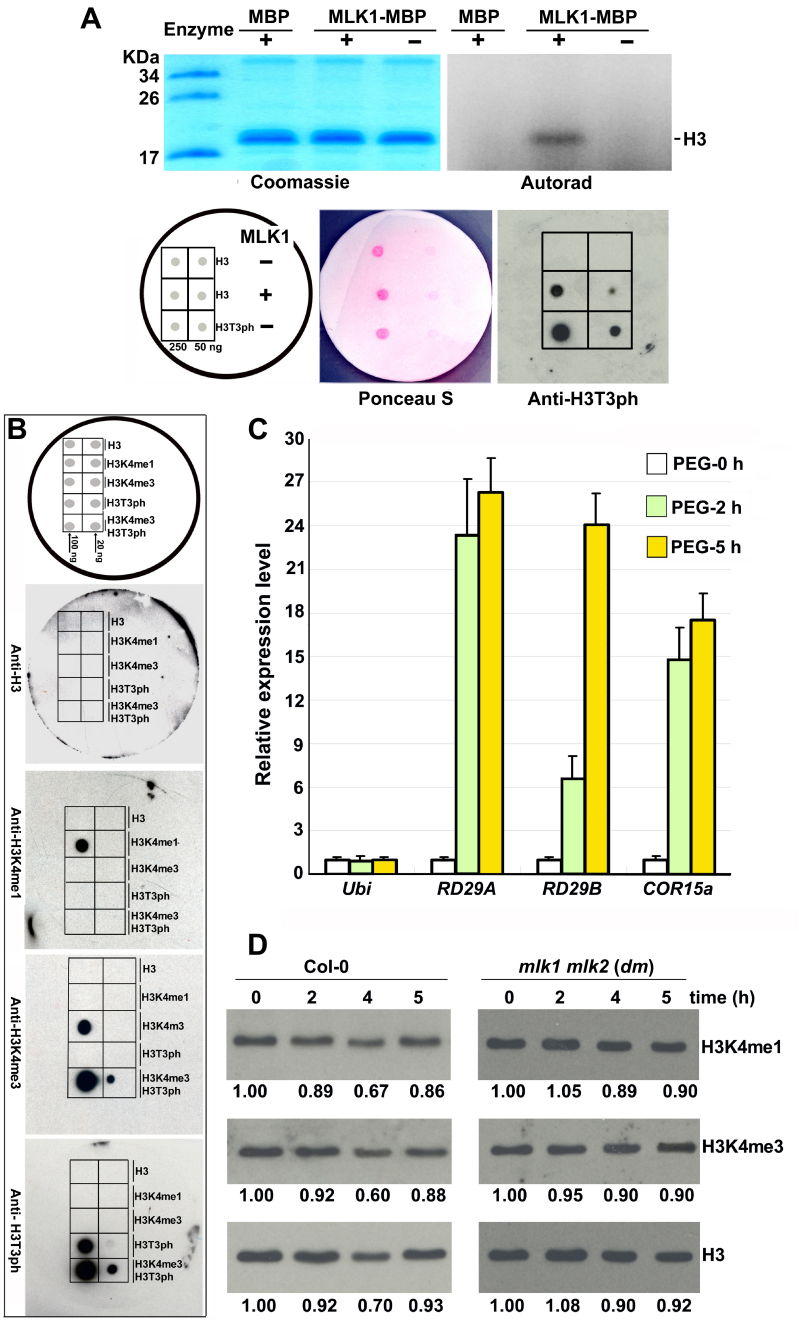

Fig. S3. Phosphorylation activity of MLK1, antibody specificity test, transcriptional analysis of drought-responsive marker genes, and methylation status of histone H3 lysine 4 under PEG treatment. (*A*) Recombinant MLK1-MBP fusion protein activity on calf thymus histone H3 (upper panels) or on an unmodified histone H3 peptide (residues 1-21) (bottom panels). Reactions were carried out in liquid medium (in the presence or absence of MLK1-MBP), then peptides were spotted on a nitrocellulose filter and peptide modification was examined by immunoblotting with an anti-H3T3ph antibody (see *B* for peptide descriptions and antibody characterization). (*B*) Examination of the specificity of the antibodies used in this study by dot blotting. The indicated amounts of each peptide were spotted on nitrocellulose filters (Whatman 7182-004) and immunodetected separately with individual antibodies. H3, unmodified histone H3 peptide (residues 1-21), biotin conjugate (Upstate 12-403); H3K4me1, monomethyl-histone H3 (Lys4) peptide (residues 1-21), biotin conjugate (Upstate 12-563); H3K4me3, trimethyl-histone H3 (Lys4) peptide (residues 1-21), biotin conjugate (Upstate 12-564); H3T3ph, phospho-histone H3 (Thr3) peptide (residues 1-21), biotin conjugate, synthesized by BIOMATIK Corporation; and H3K4me3/H3T3ph, trimethyl(Lys4)-phospho(Thr3) histone H3 peptide (residues 1-21), biotin conjugate, synthesized by BIOMATIK Corporation. Note that the anti-H3 antibody (Abcam, ab1791) was raised against the carboxyl-terminal end of histone H3 and therefore does not recognize any of these peptides. (*C*) Real time PCR analysis of transcript levels of drought-inducible marker genes in wild type Arabidopsis plants exposed to 30% PEG. Data were normalized to *POLYUBIQUITIN 10* (*At4g05320* = *Ubi*) and plotted relative to transcript levels in plants grown under normal conditions (PEG-0 h). Values shown are the mean +/- SD of three independent experiments. (*D*) Immunoblot analysis of mono- and tri-methylation of histone H3 at lysine 4 (H3K4me1 and H3K4me3) in the wild type and the *dm* exposed to 30% PEG for the indicated times. Histone H3 levels were also examined to verify equivalent loading of the lanes.

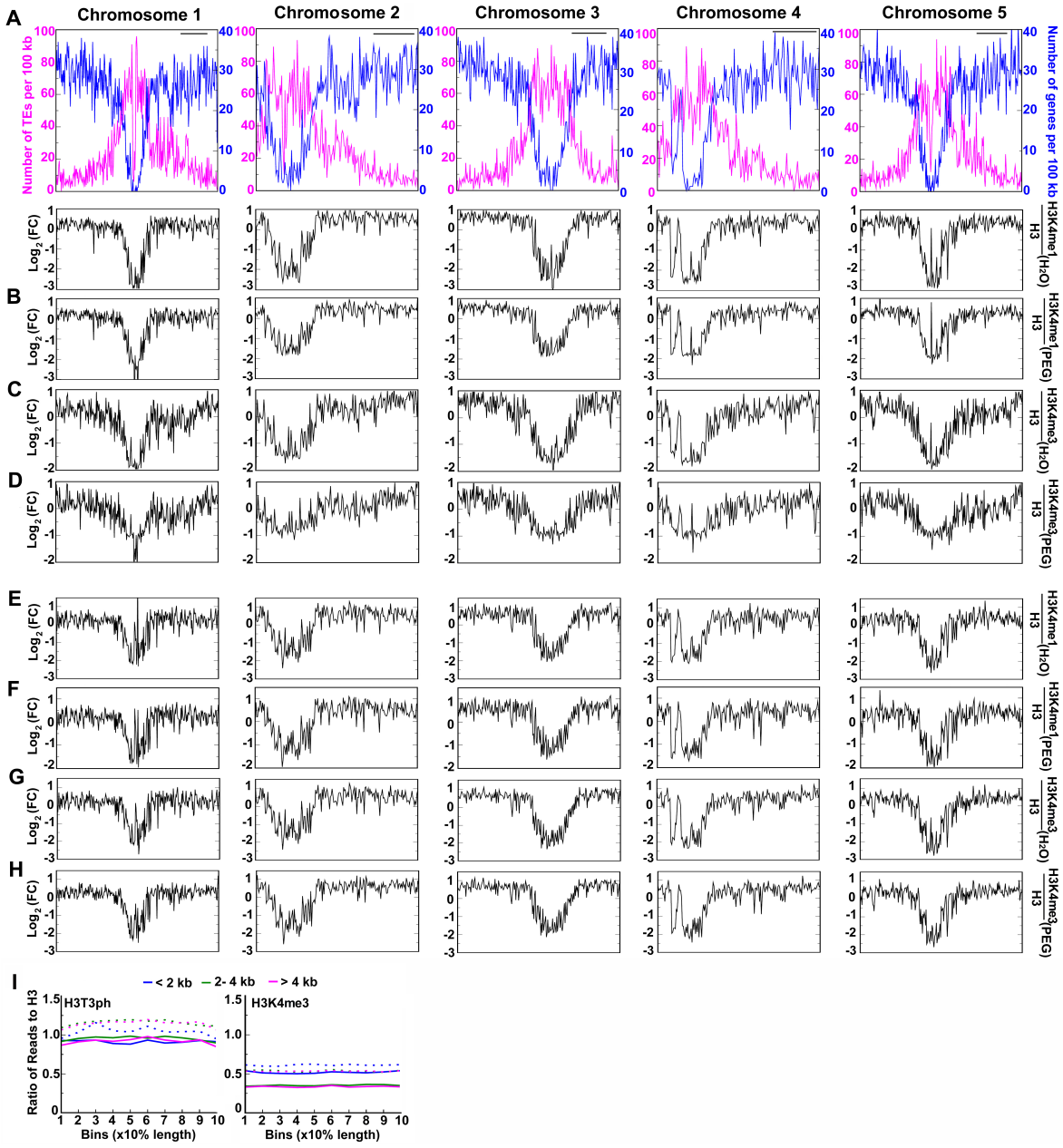

Fig. S4. Genome-wide distribution of H3K4me1 and H3K4me3 in wild-type Arabidopsis and the *mlk1 mlk2* double mutant. (*A*) Chromosomal distribution of genes (blue) and transposable elements (TEs) (pink). Horizontal bar = 5 Mb. The lower panels indicate the chromosomal distribution, in wild type plants grown under normal environmental conditions, of H3K4me1 normalized to histone H3. The binary logarithm of the fold change (FC), average of two independent experiments, is shown. (*B-D*) Chromosomal distribution of H3K4me1 or H3K4me3 normalized to histone H3 abundance in wild type plants grown under the conditions indicated on the right axis. (*E-H*) Chromosomal distribution of H3K4me1 or H3K4me3 normalized to histone H3 abundance in *dm* plants grown under the conditions indicated on the right axis. (*I*) Distribution of H3T3ph and H3K4me3 within TEs of different lengths in wild type plants. Solid and dashed lines represent the distribution under normal conditions and after 5 h PEG treatment, respectively.

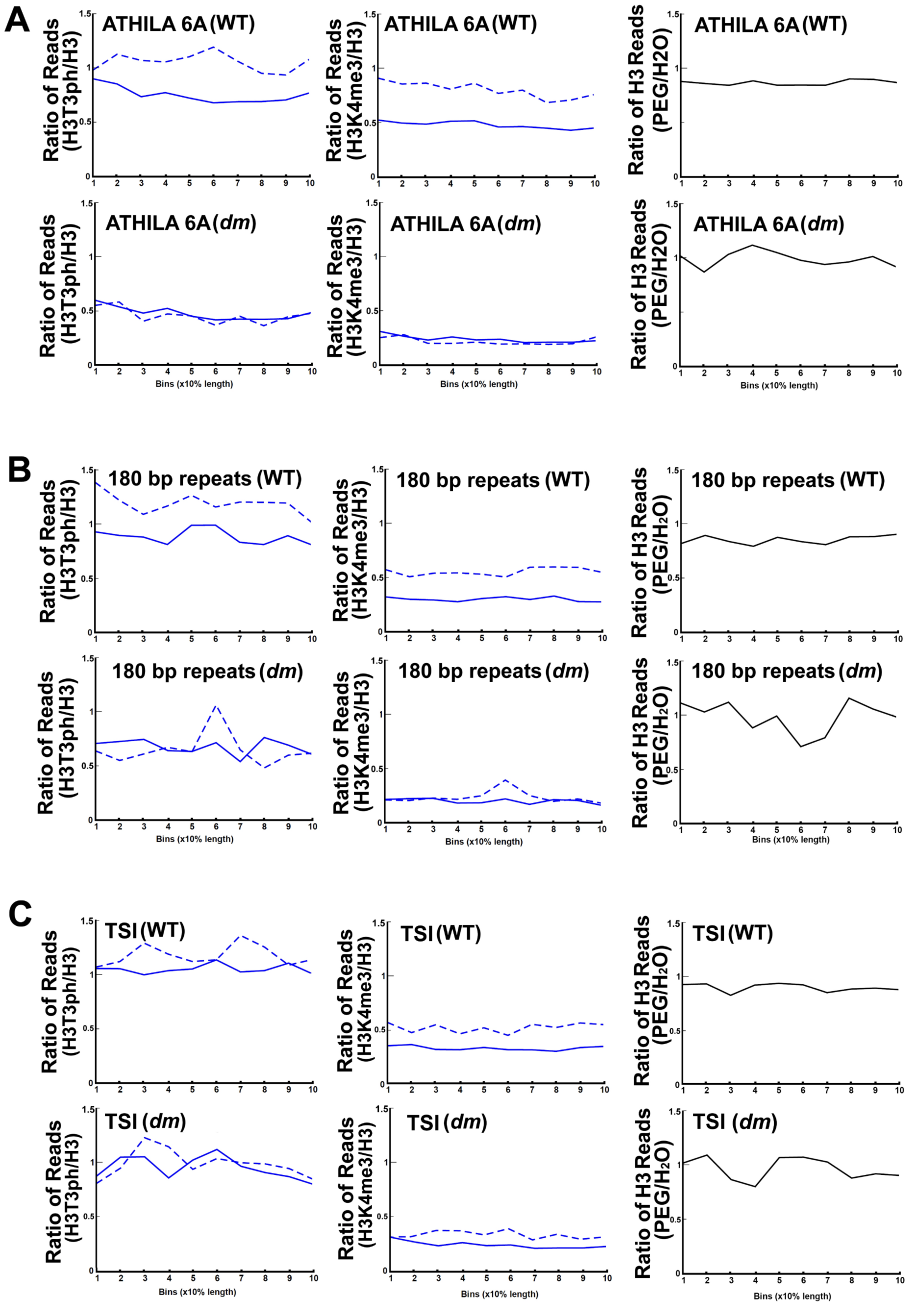

Fig. S5. Distribution of H3T3ph and H3K4me3 within the indicated transposable elements and repeats in wild type (WT) and *mlk1 mlk2* (*dm*) mutant plants grown under different environmental conditions. The abundance of histone H3 in PEG treated plants relative to that in well-watered controls is also shown. Solid blue line, plants grown under well-watered conditions. Dashed blue line, plants exposed to 30% PEG for 5 h. (*A*). Distribution of H3T3ph and H3K4me3 within the *ATHILA6A* transposon. (*B*). Distribution of H3T3ph and H3K4me3 within centromeric 180 bp repeats. (*C*). Distribution of H3T3ph and H3K4me3 within the *TRANSCRIPTIONALLY SILENT INFORMATION* (*TSI*) locus.

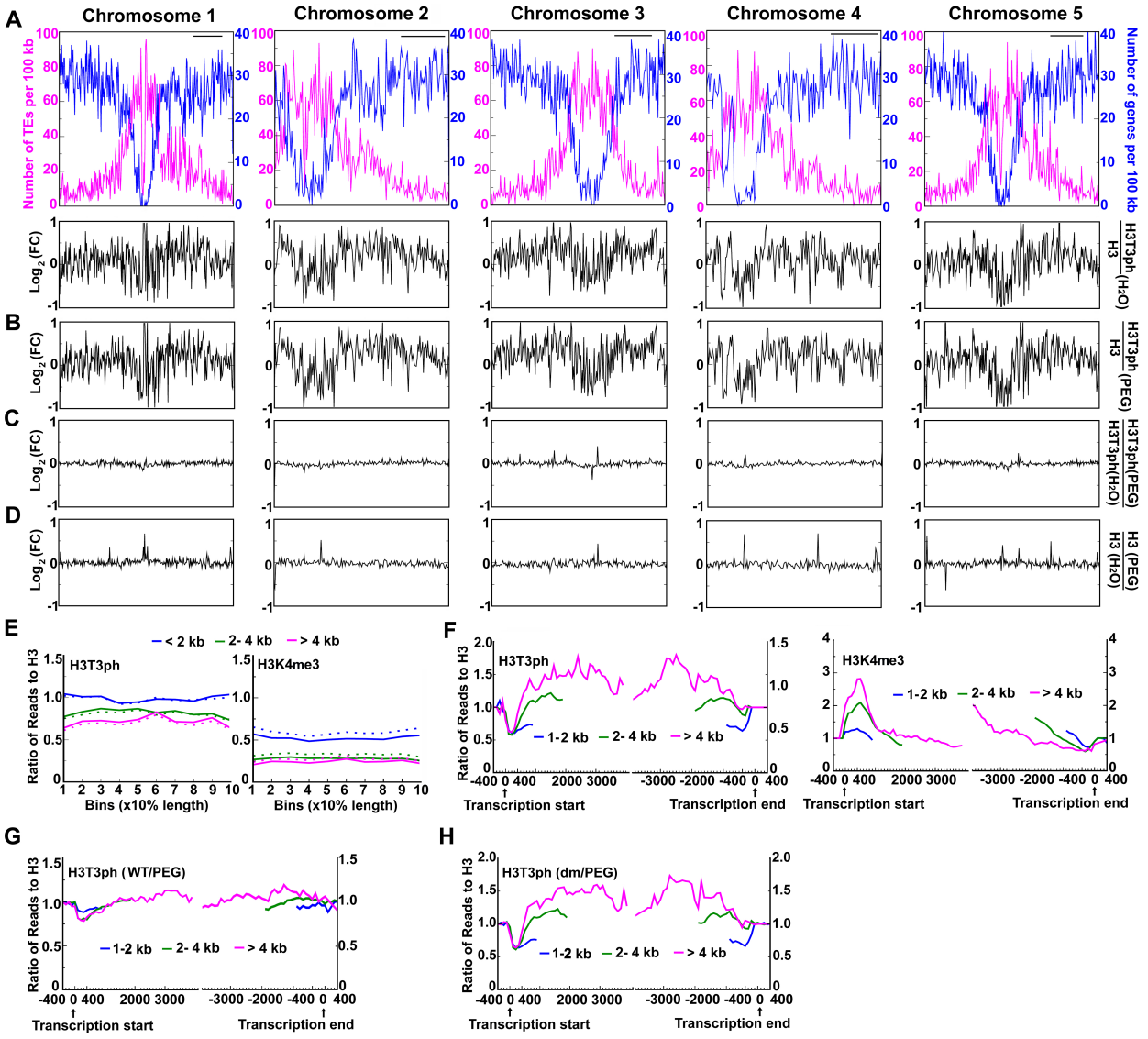

Fig. S6. Chromosomal distribution of H3T3ph in the *mlk1 mlk2* double mutant. (*A*) Chromosomal distribution of genes (blue) and transposable elements (TEs) (pink). Horizontal bar = 5 Mb. The lower panels indicate the chromosomal distribution under normal environmental conditions of H3T3ph normalized to histone H3. The binary logarithm of the fold change (FC), average of two independent experiments, is shown. (*B-C*) Chromosomal distribution of normalized H3T3ph in plants grown under the conditions indicated on the right axis. (*D*) Chromosomal distribution of histone H3 in PEG treated plants relative to that in well-watered controls. (*E*) Distribution of H3T3ph and H3K4me3 within TEs of different lengths. Solid and dashed lines represent the distribution under normal conditions and after 5 h treatment with 30% PEG, respectively. (*F*) Distribution of H3T3ph and H3K4me3 in transcriptionally active protein-coding genes in plants grown under normal environmental conditions. Genes were aligned at the transcription start sites or transcription end sites within each length group. The ratio of reads was determined at 100-bp intervals. (*G*) Distribution of H3T3ph in transcriptionally active protein-coding genes in wild type plants exposed to 30% PEG (This is the only panel in the figure presenting data from wild type Col-0 plants). (*H*) Distribution of H3T3ph in transcriptionally active protein-coding genes in *dm* plants exposed to 30% PEG.

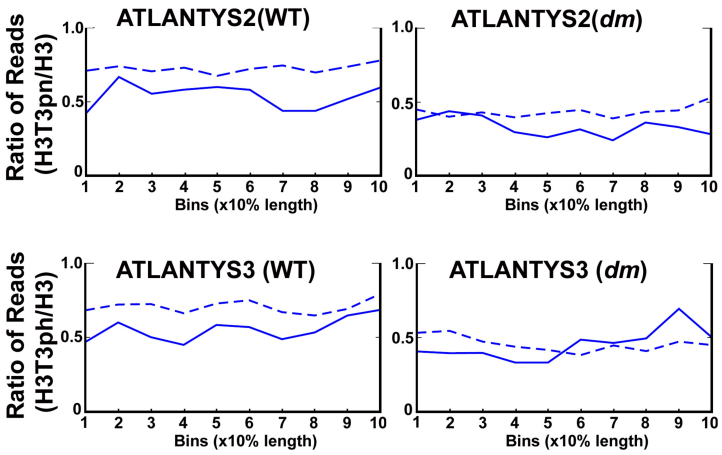

Fig. S7. Distribution of H3T3ph within the indicated TEs in wild type (WT) and *mlk1 mlk2* (*dm*) mutant plants grown under normal environmental conditions. Dashed lines represent transposable element copies located in pericentromeric regions and solid lines indicate transposable element copies located in gene-rich chromosome arms. *Atlantys* belongs to the *Ty3-gypsy* class of Long Terminal Repeat retrotransposons.

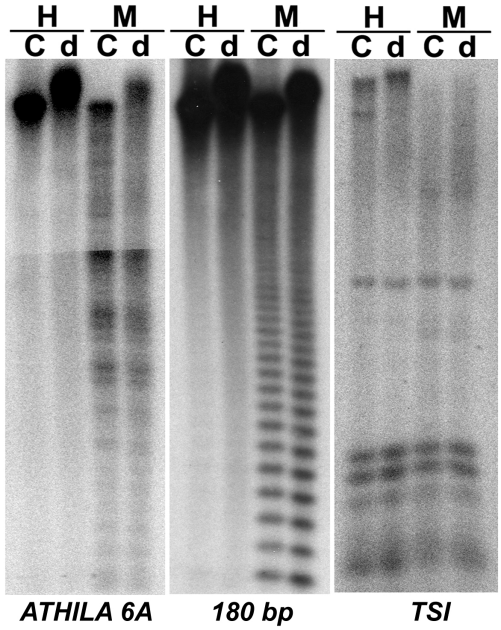

Fig. S8. DNA methylation status of the indicated loci. *180 bp*, centromeric 180bp repeats; *TSI*, *TRANSCRIPTIONALLY SILENT INFORMATION* element. Genomic DNA of Col-0 (**C**) and the *dm* (**d**) was digested with methylation–sensitive restriction endonucleases H*pa*II (H) and M*sp*I (M), which are mainly sensitive to methylation in the CG and CHG contexts, respectively. Southern blot analysis was performed with probes specific to each locus.

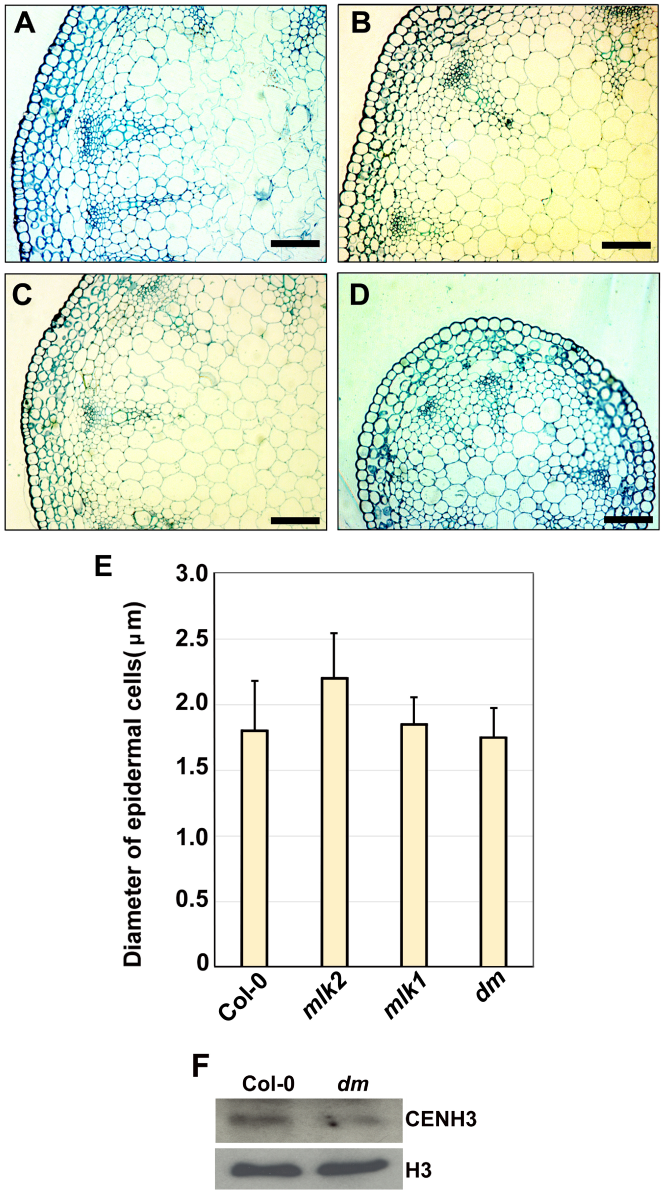

Fig. S9. Comparison of cell size in stems and immunoblot analysis of CENH3 abundance. (*A-D*) Basal regions of stems from three-week old plants were dissected and fixed in 2% formaldehyde. After embedding in resin, 1-µm-thick transverse sections were examined by light microscopy. Bar = 10 µm. Strains: Col-0 (*A*), *mlk2* mutant (*B*), *mlk1* mutant (*C*), and *mlk1 mlk2* (*dm*) double mutant (*D*). (*E*) Average diameter (+/- SD) of epidermal cells from stems of the indicated lines. (*F*) Western blot analysis of CENH3 levels in the indicated strains grown under well-watered conditions.

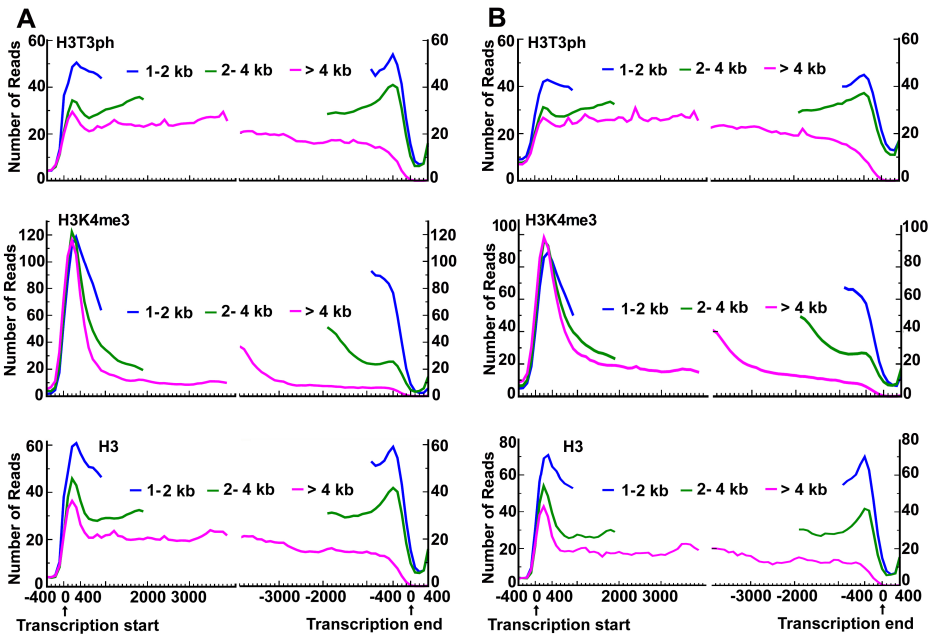

Fig. S10. Distribution of raw reads for H3T3ph, H3K4me3, or H3 within expressed protein-coding genes in wild type (*A*) and the *mlk1 mlk2* double mutant (*B*) under normal growth conditions. Genes, classified within three groups by length, were aligned at the transcription start sites or transcription end sites. Read counts were determined at 100-bp intervals.

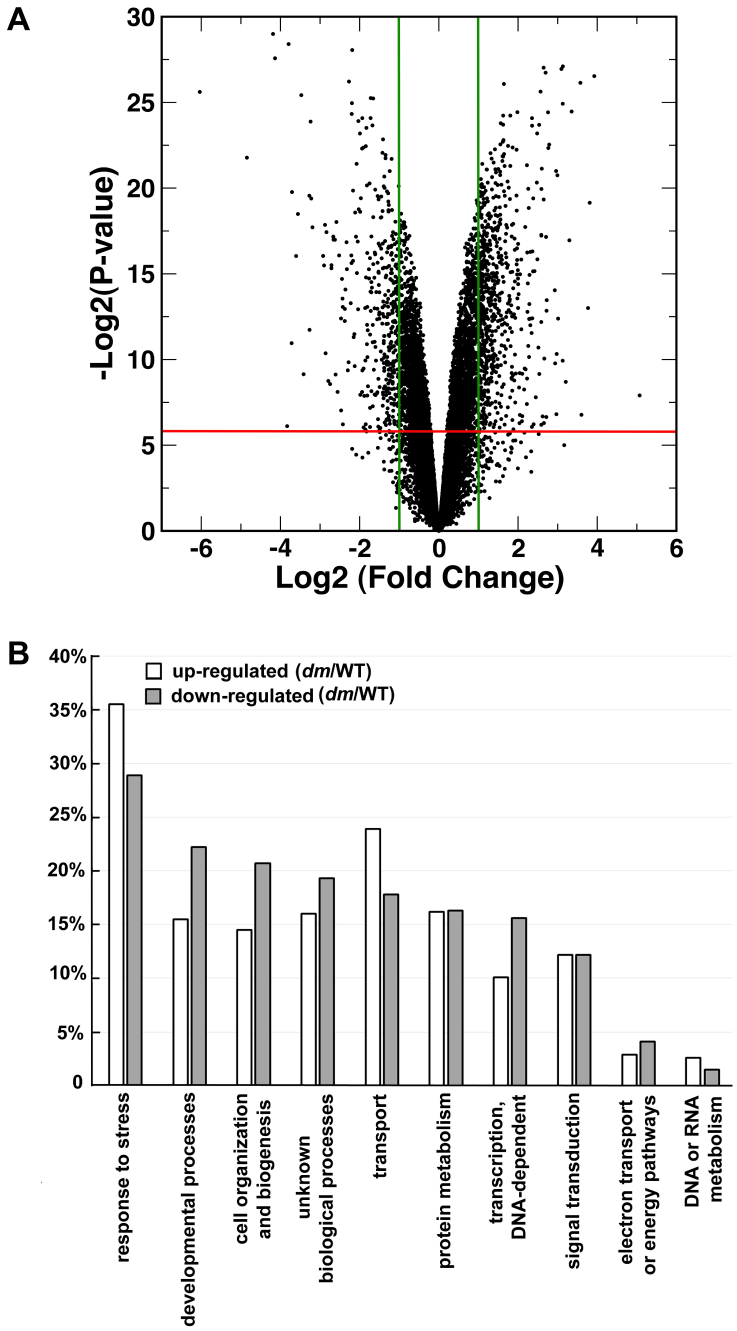

Fig. S11. Transcriptome analysis of differentially expressed genes in the *mlk1 mlk2* double mutant relative to the Col-0 wild type. (*A*) Volcano plot of differentially expressed genes. The horizontal red line indicates the significance threshold (P value = 0.01) and the vertical green lines indicate the twofold change in transcript abundance thresholds. By these criteria, 543 genes were up-regulated and 270 genes were down-regulated in the mutant background (Dataset S1), representing ~3% of the annotated Arabidopsis protein coding genes. (*B*) Functional categorization of differentially expressed genes based on gene ontology (GO) annotations. About one third of the differentially expressed genes are annotated as being involved in responses to stress.

Table S1. Correlation coefficients between two biological replicate libraries, for each epigenetic mark examined and for each experimental condition, from wild type plants.

	Treatment	Chrom 1	Chrom 2	Chrom 3	Chrom 4	Chrom 5	Average
H3T3ph	H_2O Control	0.79	0.85	0.83	0.89	0.83	0.84
	5 h PEG	0.83	0.82	0.77	0.79	0.83	0.81
H3K4me1	H_2O Control	0.99	0.99	0.99	0.98	0.99	0.99
	5 h PEG	0.99	0.99	0.99	0.99	0.99	0.99
H3K4me3	H_2O Control	0.98	0.98	0.98	0.98	0.98	0.98
	5 h PEG	0.95	0.90	0.94	0.89	0.90	0.92
Histone H3	H_2O Control	0.92	0.95	0.93	0.95	0.95	0.94
	5 h PEG	0.88	0.92	0.92	0.94	0.91	0.91

Note: For the analysis of correlation coefficients, after a least-squares fitting, calculations were conducted between the two sets of normalized reads from two biological libraries at every 100 kb intervals of the reference genome. Correlation coefficients were calculated separately for individual chromosomes (Chrom).

Table S2. P-values of T-tests between pericentromeric regions and random euchromatic regions of similar length on each chromosome.

	Chromosome 1 (12.4 – 17.6 Mb)	**Chromosome 2 (1.6 – 6.7 Mb)**	**Chromosome 3 (11.0 – 16.2 Mb)**	**Chromosome 4 (1.6 – 5.7 Mb)**	**Chromosome 5 (9.9 – 14.6 Mb)**
H3T3ph distribution under normal growth conditions normalized to H3 (Fig. 3A)					
Peak vs Ctl 1	0.066645291	0.462570402	0.190486371	0.076289893	0.007432076
Peak vs Ctl 2	0.003916099	0.007339557	0.022405097	0.034582019	0.001874103
Ctl 1 vs Ctl 2	0.219477933	0.057632076	0.195797609	0.612536661	0.670045552
H3T3ph distribution under PEG treatment normalized to H3 (Fig. 3B)					
Peak vs Ctl 1	2.87037E-07*	2.06966E-13*	9.54308E-12*	2.23693E-07*	4.25192E-06*
Peak vs Ctl 2	1.84132E-06*	2.06029E-09*	1.06028E-14*	3.86627E-06*	6.3236E-05*
Ctl 1 vs Ctl 2	0.657569369	0.001374072	0.485728373	0.29972716	0.141025684
H3T3ph distribution under PEG normalized to H3T3ph under normal conditions (Fig. 3C)					
Peak vs Ctl 1	1.43921E-09*	3.81325E-14*	1.96539E-11*	1.12886E-09*	3.66864E-13*
Peak vs Ctl 2	8.77581E-12*	1.9666E-16*	1.3067E-17*	1.11986E-08*	8.77298E-14*
Ctl 1 vs Ctl 2	0.076683586	0.272274073	0.007696669	0.519306034	0.356186221
H3 distribution under PEG normalized to H3 under normal conditions (Fig. 3D)					
Peak vs Ctl 1	1.37333E-09*	5.98035E-07*	5.00246E-05*	3.34386E-08*	4.40776E-07*
Peak vs Ctl 2	2.83694E-14*	1.09549E-08*	1.45039E-05*	1.57887E-08*	5.32232E-10*
Ctl 1 vs Ctl 2	0.000847258	0.000695802	0.054428738	0.621822066	0.002424166

Note: The area of highest transposon element density on each chromosome was defined as a pericentromeric region (Peak). Two areas of the same length, but located in regions of low transposon density (euchromatic regions), were randomly selected as Control 1 (Ctl 1) and Control 2 (Ctl 2) on each chromosome. To determine whether the relative abundance of H3T3ph or H3 in pericentromeric (Peak) regions differed significantly from that in euchromatic (Control) regions under a given condition, the values in a peak area and in a control area were compared by T-test. *P< 0.0001 was considered indicative of a significant difference between Peak and Control regions on the same chromosome.

Table S3. Sequences of primers used in this study.

RT-PCR	
UBIQUITIN 10	Forward: 5'- AGGATGGCAGAACTCTTGCT-3'; Reverse: 5'-TCCCAGTCAACGTCTTAACG-3'
RD29A	Forward: 5'- AGGAACCACCACTCAACACA-3'; Reverse: 5'- ATCTTGCTCATGCTCATTGC-3'
RD29B	Forward: 5'- ACGAGCAAGACCCAGAAGTT-3'; Reverse: 5'- AGGAACAATCTCCTCCGATG-3'
COR15a	Forward: 5'- CAGATGGTGAGAAAGCGAAA-3'; Reverse: 5'- CCCTACTTTGTGGCATCCTT-3'
180-bp repeats	Forward: 5'-ACCATCAAAGCCTTGAGAAGCA-3'; Reverse: 5'-CCGTATGAGTCTTTGTCTTTGTATCTTCT-3'
TSI	Forward: 5'- CTCTACCCTTTGCATTCATGAATCCTT-3'; Reverse: 5'-GATGGGCAAAAGCCCTCGGTTTTAAAATG-3'
Athila-6A	Forward: 5'-CAGGTCGAGTAACCTCAGGTCA-3'; Reverse: 5'-GAGTAACTTGGTAGAGTGAATGGTC-3'
Ta3LTR	Forward: 5'-TAGGGTTCTTAGTTGATCTTGTATTGA-3'; Reverse: 5'-TTTGCTCTCAAACTCTCAATTGAAGTT-3'
MLK1	Forward: 5'-GCG GCATAAGGTATGCAAGTGTT-3'; Reverse: 5'-GCGACTGAGATCCACTGACAA-3'
MLK2	Forward: 5'-GATCGAGACGCCTTGACGAGC-3'; Reverse: 5'-CAGGTTCAGTGGCCCCTATAG-3'
MLK3	Forward: 5'-TGGATCAGCATTTACAGTGCTCACAGAC-3'; Reverse: 5'-TCCACTTGAAGGGAAAAGAATCACTGAC-3'
MLK4	Forward: 5'-AGTGGAGAGAAGGTGGTAGCGGAC-3'; Reverse: 5'-GCGATGTTGCCATCTTCTTTTTGC-3'
Genotyping	
MLK1	Forward: 5'-CCATGGCAAGGATATCAGGTCTGTTTTT-3'; Reverse: 5'-AATAAAAATGGCATTAAACCGGGGTGAG-3'
MLK2	Forward: 5'-ACATCAAACAAGGTTTGTGCATGGAGAT-3'; Reverse: 5'-TATTCGTAACTGCCTCGAGGAACAGCTT-3'
MLK3	Forward: 5'-TGGATCAGCATTTACAGTGCTCACAGAC-3'; Reverse: 5'-TCCACTTGAAGGGAAAAGAATCACTGAC-3'
MLK4	Forward: 5'-AGTGGAGAGAAGGTGGTAGCGGAC-3'; Reverse: 5'-GCGATGTTGCCATCTTCTTTTTGC-3'
T-DNA borders	AtLB21: 5'- TGGTTCACGTAGTGGGCCATCG-3'; 8603RB R1: 5'-CCCATTTGGACGTGAATGTAGACAC-3'
Constructs	
MLK1-GFP	Forward: 5'- CACCATGCCAGAGTTAAGAAGTGGAGCA-3'; Reverse: 5'- GCAAACTGTCCTCCCAAAGCATATTGA-3'
Complementation	Forward: 5'-GGATCCATGCCAGAGTTAAGAAGTGGACGT-3';Reverse: 5'-GGTACCTCAGCAAACTGTCCTCCCAAA-3'
MLK1-kinase	Forward: 5'- GGGCGGCCGCATGCCAGAGTTAAGAAGT-3'; Reverse: 5'-GCGGATCCGCAAACTGTCCTCCCAAAGC-3'